NASA

# DEVELOPMENT OF A 3400 WATT PROGRAMMED DC POWER SUPPLY PROVIDING STATIC AND DYNAMIC SOLAR CELL ARRAY SIMULATION

by

Paul Knauer

prepared for

## NATIONAL AERONAUTICS AND SPACE ADMINISTRATION

Contract NAS 3-7920

WESTINGHOUSE ELECTRIC CORPORATION
AEROSPACE ELECTRICAL DIVISION
LIMA, OHIO

SUMMARY REPORT

# DEVELOPMENT OF A 3400 WATT PROGRAMMED DC POWER SUPPLY PROVIDING STATIC AND DYNAMIC SOLAR CELL ARRAY SIMULATION

by

Paul Knauer

prepared for

## NATIONAL AERONAUTICS AND SPACE ADMINISTRATION

Contract NAS 3-7920

November 15, 1966

DEVELOPMENT OF A 3400 WATT
PROGRAMMED DC POWER SUPPLY
PROVIDING STATIC AND DYNAMIC
SOLAR CELL ARRAY SIMULATION


by


Paul Knauer


## ABSTRACT

The primary objective in the design of the solar-cell array sim-
ulator was to provide a source of d-c power which would be sim-
ilar, both statically and dynamically, to the output of a solar-
cell array. To accomplish the latter, a large number of parallel
power transistors operated as a Class-A series regulator were
employed as the main controlling element. The solar-cell array
volt-ampere characteristics were obtained by utilizing a diode
function generator. The simulator operates in a closed-loop
mode incorporating both voltage and current feedback. The re-
sulting transient response obtained in the simulator is in the
order of 50 microseconds.

## TABLE OF CONTENTS

## LIST OF ILLUSTRATIONS

## LIST OF ILLUSTRATIONS (Continued)

DEVELOPMENT OF A 3400 WATT
PROGRAMMED DC POWER SUPPLY
PROVIDING STATIC AND DYNAMIC
SOLAR CELL ARRAY SIMULATION

by

Paul Knauer


Westinghouse Electric Corporation
Lima, Ohio

## SUMMARY


The purpose of this project was to develop a programmed d-c power
supply capable of reproducing both the static and the dynamic
characteristics of a solar-cell array. Simulation of the static
characteristics was straightforward. The volt-ampere character-
istics were determined by a diode-resistor function generator.
Simulation of the dynamic characteristics, however, was one of
the major design problems.

In order to obtain a transient response similar to that of a
solar-cell array, a number of parallel power transistors were
operated in a Class-A series regulator mode. This configuration
eliminated the need for large filters normally associated with
pulse-width-modulated control elements, and their inherent slow
response. Consequently, the response time exhibited by the com-
plete simulator was approximately 50 microseconds.

The quantity of parallel transistors was determined by the maxi-
mum power dissipation requirement of the supply, in this case
2500 watts. An efficient heatsink assembly utilizing forced-air
cooling was used to minimize the number of transistors to 25.

Good engineering practice dictated that the simulator should be
self-protecting. To this end, a power sensor was employed in a
unique configuration which electrically maintained the power
transistor dissipation below a safe value.

## INTRODUCTION

The primary objectives of contract NAS3-7920 were twofold.

1. To develop power conditioning equipment to control and operate a Cesium Electron Bombardment Ion Thrustor System capable of operating from a solar-cell array energy source. (See NASA report CR-54672.)

2. To develop a power supply which would simulate, as closely as possible, the static and dynamic output characteristics of a solar-cell array, thereby allowing complete systems testing.

This report covers the second item only.

The completed power supply performs the intended functions well and, in addition, is self-protecting against static and transient load conditions of any kind. Illustrations which may be of immediate interest are:

Figure 1. Output Volt-Ampere Characteristics.
Figure 8. Photograph of Typical Transient Response Waveforms.
Figure 12. Photograph of Complete Unit.


## BACKGROUND

The static output characteristic range and capability which were to be simulated are shown in figure 1. From this figure, it was apparent that load currents exceeding 80 amperes could be expected. In order to control currents of this magnitude, a pulse-width-modulated approach was considered from an efficiency standpoint. Pulse-width-modulated control may be obtained by using transistors, while thyristors would perform equally well. In either case, an appropriate L-C filter would be necessary to provide a smooth d-c output.

The closed-loop frequency response of a system utilizing pulse-width-modulation is inherently limited by the output filter, especially when load transients are such as to cause the regulator to attempt operation outside of its control limits, e.g., 100 percent duty cycle. Attempts to raise the closed-loop response by increasing the regulator switching frequency would require switching in the range of 100-200 kHz. This was considered to be extremely difficult in view of the present state-of-the-art.
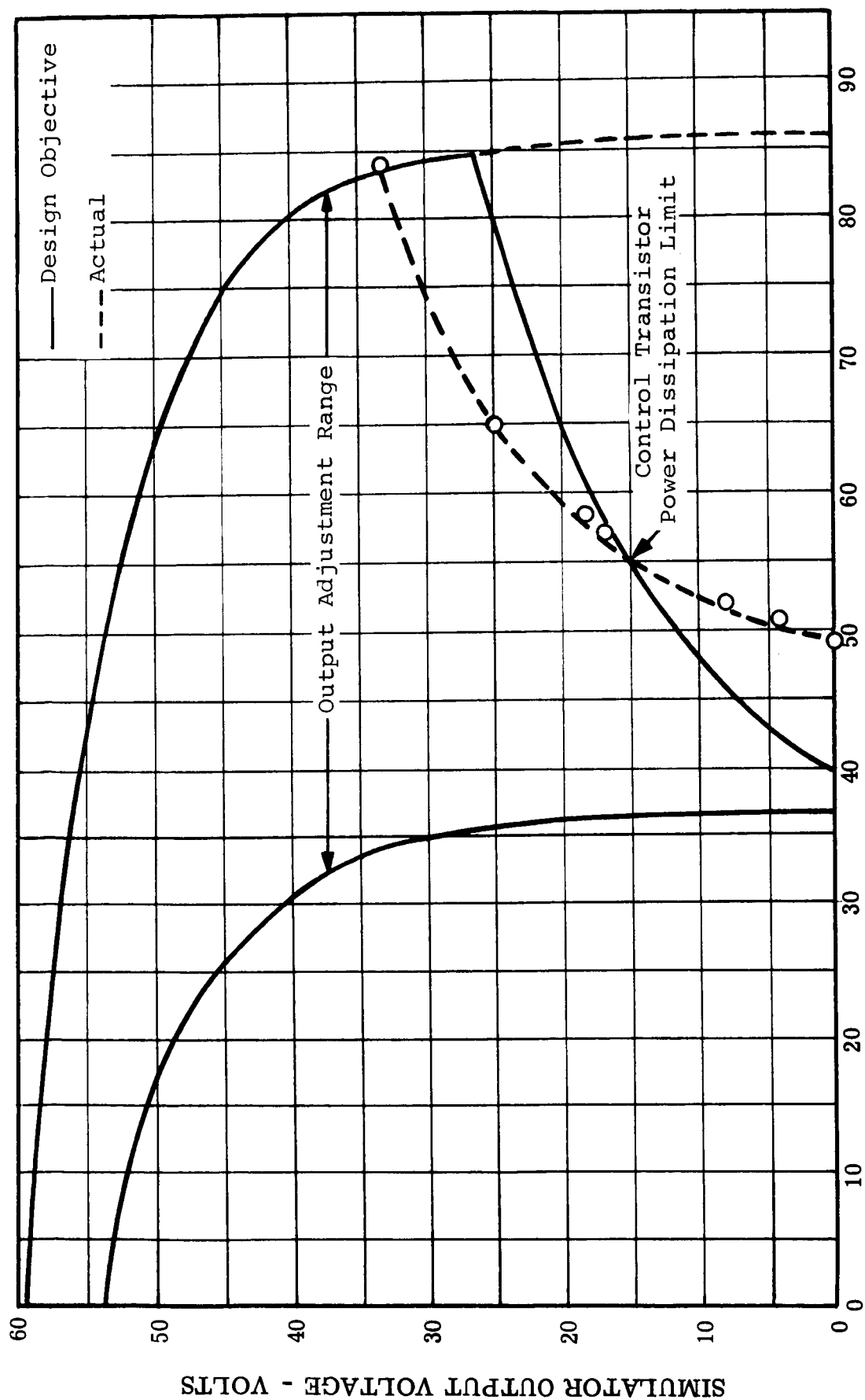
SIMULATOR OUTPUT CURRENT - AMPERES

FIGURE 1. Solar Cell Simulator Output Characteristics

3

To overcome the frequency response limits imposed by an output filter, a power stage operated in a Class-A mode was investigated. The response time of a regulator of this type was limited by the transistors themselves, since an external filter was not required, and was therefore capable of considerably faster response. The main objection to this arrangement, of course, was the power dissipation requirement imposed upon the series control transistor. Referring to figure 1, dissipation in this transistor, under short-circuit conditions, is the product of the open-circuit voltage and the short-circuit current. In the design under consideration, the product exceeded 5000 watts.

A compromise between the pulse-modulated approach and the Class-A approach, a possible method of reducing this high dissipation, would be to incorporate thyristor control and Class-A transistor control in a series mode. In this manner, the transistors would allow rapid control over small load excursions, while the thyristor element with its associated filters would provide the coarse control required over large load excursions. Since this restricts the magnitude of the allowed load excursions, the Class-A series transistor approach was selected as the main controlling element.

## THE SIMULATOR POWER STAGE

The simulator was expected to follow closely the solar-cell array characteristics during power conditioner tests, especially under short-circuit current conditions. At times, however, it may be desirable to operate two power conditioners from this supply, although no short-circuit tests would be conducted under these conditions. Both requirements are fulfilled by the simulator, as demonstrated by the characteristics curves shown in figure 1. In this approach, the power dissipation requirements of the series control transistors are held to a minimum by sensing and limiting the dissipation with a closed-loop control arrangement.

Thus simulator operation with only one power conditioner, which would require a short-circuit capability somewhat less than 40 amperes, would not enter the power-dissipation-limit region of the characteristics curve. The capability of operation with two power conditioners is also maintained past the maximum-power point, where normal operation can be maintained.

The transistor power-dissipation capability utilizing this approach was 2500 watts. A parallel transistor approach was considered feasible only if the transistors could be forced to share load current. (This was ultimately accomplished by the addition of a low-value resistor into the emitter circuit of each of the paralleled transistors to provide sufficient current feedback to ensure current sharing.)

4

In order to employ as few transistors as possible, the transistors were selected on the basis of power dissipation capability. This required, in general, a transistor with a high current capacity, since a higher current requires a large semiconductor chip, which, by its very size, is capable of conducting heat to the transistor case more rapidly. Consequently, a Westinghouse type 2N2758 transistor was selected. Rated at 30 amperes, this transistor can safely dissipate 100 watts at a case temperature of 100° C. Under these conditions, the transistor junction temperature remains below 150° C, or 25° C below its rated temperature. Twenty-five parallel transistors of this type were required to form the main regulator controlling element. These transistors are designated Q101 through Q125 in the schematic diagram shown in figure 2. Note that each transistor has an associated series fuse. Should any of the paralleled transistors fail shorted, that transistor would attempt to carry the entire load current. If this were to happen, the 5-amp fuse associated with the failed transistor would open, thereby removing the transistor from the line, and providing a visual indication of the failed transistor.

## CONTROL PHILOSOPHY

Transistors Q1 through Q4 provide the current amplification required to drive the main power transistors with the low-level signal available from operational amplifier A1.

Figure 3A shows a typical operational-amplifier circuit. It can easily be verified that, if the gain of the amplifier is sufficiently high and of the proper polarity, operation of the circuit can be described by the following equation:

$$E_O = \left( \frac{Rf}{Ri_1} \right) E1 + \left( \frac{Rf}{Ri_2} \right) E2$$

In Figure 3B, a number of amplifier stages were added to the output of the amplifier A, but the equation still applies. In this circuit, however, the power output capabilities have been greatly increased.

This configuration, although somewhat simplified, is essentially derived from the schematic diagram, figure 2. Resistor R15 is the feedback resistor Rf, while R2 is input resistor $Ri_2$. Any of the potentiometers R20 through R25 are equivalent to input resistor $Ri_1$. If all the potentiometers just mentioned were removed from the circuit, then potentiometer R10 would determine

the value of $E_1$, while the ratio $\left( \frac{R16}{R2} \right)$ would determine the value

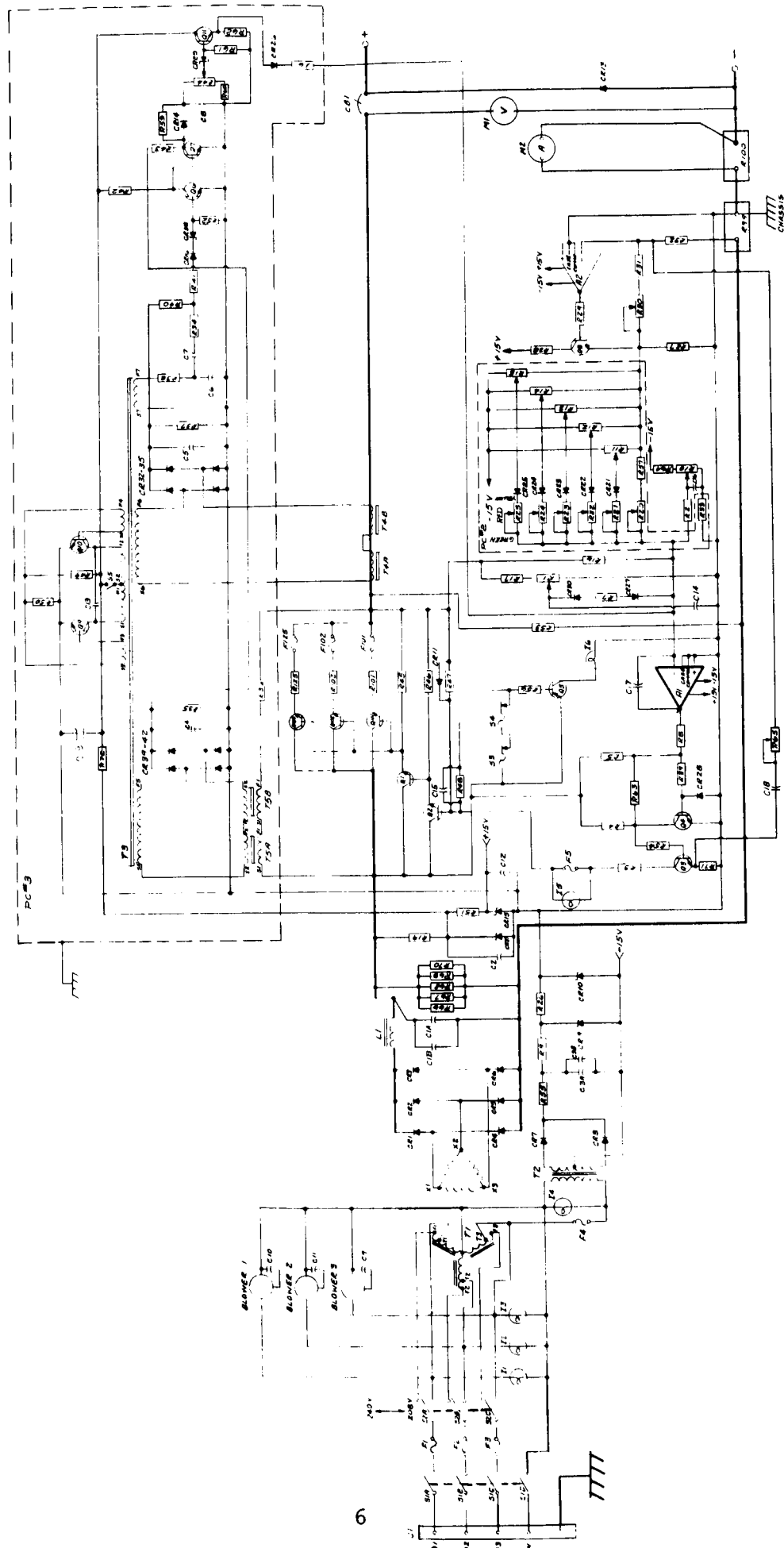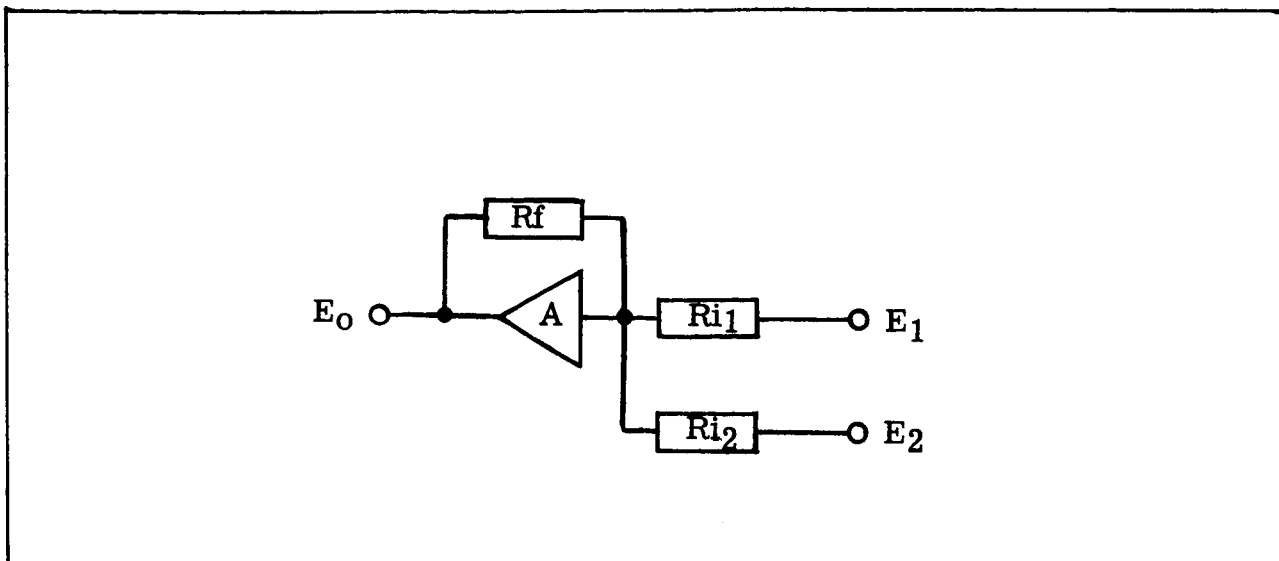**FIGURE 2. Schematic Diagram – Solar Cell Simulator**
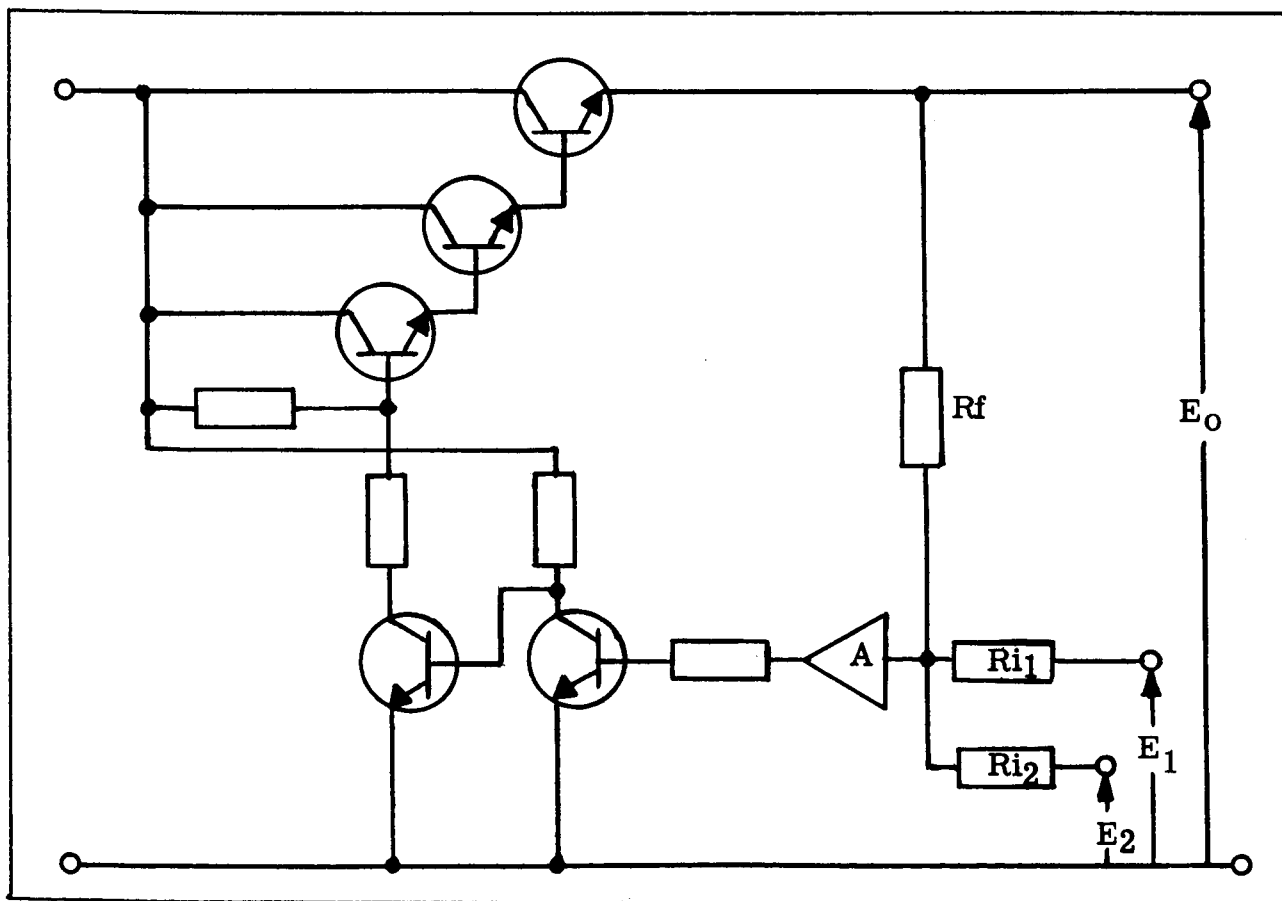
FIGURE 3A.  Typical Operational Amplifier Multiplier



FIGURE 3B.  Simplified Schematic of Power Amplifier

of $E_O$. Under this condition, the simulator would be nothing more than a voltage regulator, with $E_O$ remaining essentially constant regardless of the magnitude of the load current.

## THE FUNCTION GENERATOR

Figure 4 represents a simplified schematic diagram of the simulator's function generator. The purpose of this circuit is to provide a control voltage which will ultimately shape the output characteristic of the simulator to match that of a solar-cell array.

The voltage $E_O$ is merely a signal voltage proportional to the load current $I_L$. As long as the voltages at the taps of $R_A$ and $R_B$ are less than zero, the voltage $E_G$ remains zero. If either of the voltages exceeds "zero", or the value of $E_G$, that voltage would add to $E_G$. Thus, the relationship between $E_G$ and the load current $I_L$ in this simplified circuit would approximate the curve shown in figure 5. It now becomes apparent that a proper choice of the number of breakpoints as well as the change in slope at each of the breakpoints can result in a fairly smooth curve of the desired shape.

The function generator used in the simulator is shown in figure 2 and consists of five breakpoints, determined by potentiometers R11 through R15. The desired slope associated with each of the breakpoints is determined by potentiometers R20 through R25. Any of these potentiometers may serve as the input resistor, $R_i$, shown in figure 3B.

In figure 2, potentiometer R30 serves to control the gain of the current-sensing circuit, thereby allowing the short-circuit current of the simulator to be adjustable.

An interesting phenomena is that the required forward breakdown voltage of each of diodes CR21 through CR25, normally considered to be a less than ideal characteristic, actually serves to round off the breakpoints of the resulting function generator output, such that the discontinuities are not discernable.

## CLOSED LOOP STABILITY

The circuits described thus far form the functional part of the solar-array simulator, in that all additional circuits perform auxiliary functions such as rectification, filtering, and protection. These functions are described separately.
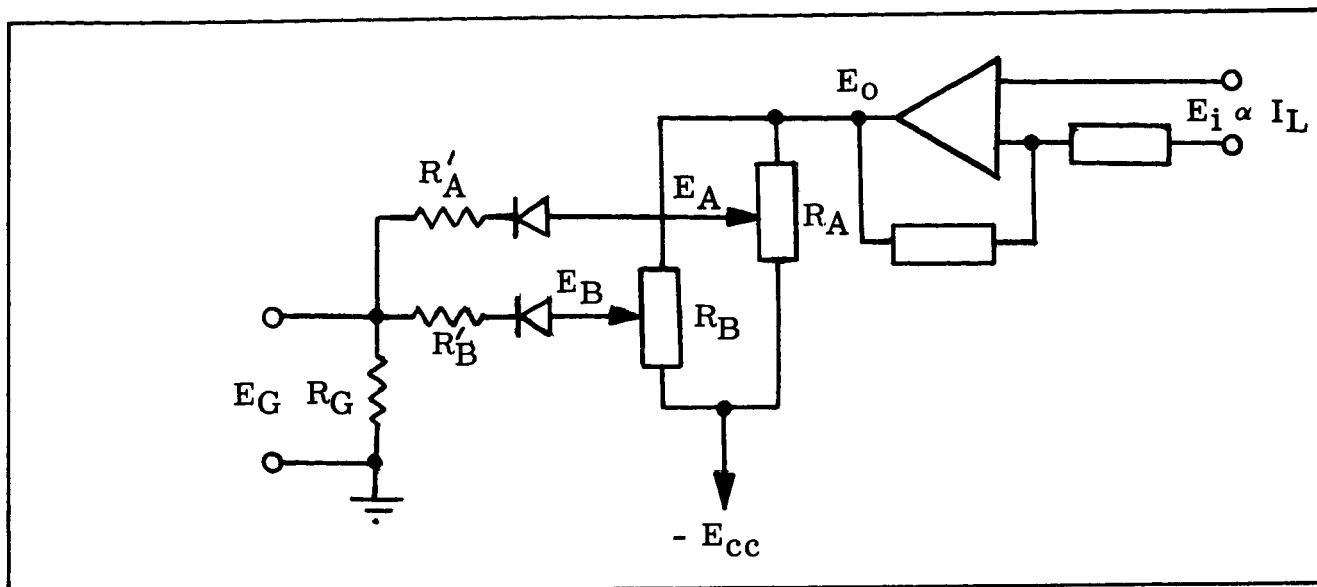
FIGURE 4. Simplified Schematic - Function Generator
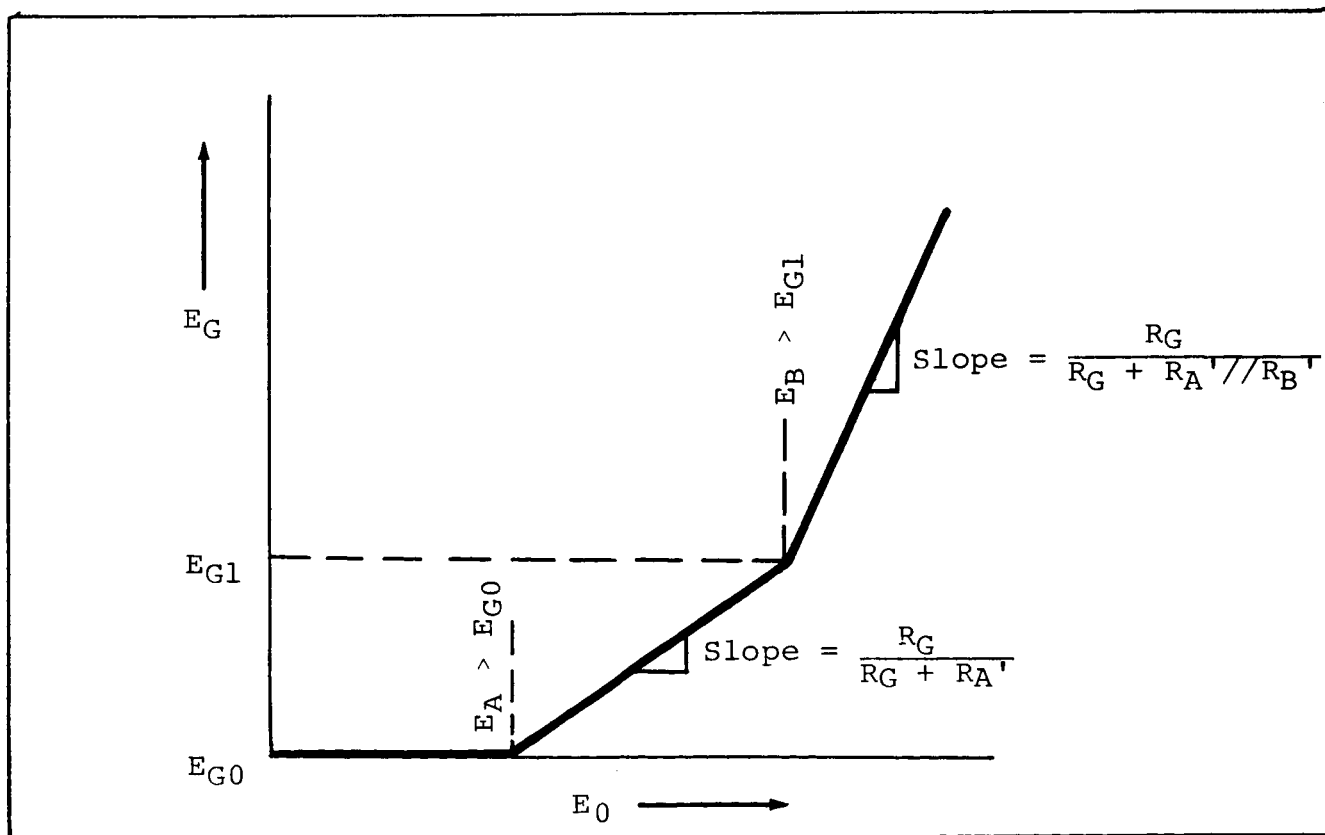


FIGURE 5. Transfer Characteristics of a Two Diode Function Generator

Stabilization of the closed loop was a greater problem than originally anticipated. An undesired closed loop was formed, for example, due to the capacitance between the various collector and base leads of transistors Q1, Q2, and the main power transistors. This loop caused oscillations within itself, which were eventually eliminated by reducing the frequency response of these transistors through the introduction of a capacitor across R48.

The main problem, however, was discovered after obtaining frequency-response curves of the simulator. These curves were obtained by disconnecting resistor R2 from R10 and capacitor C16, then applying a sinusoidal waveform of fixed magnitude to R2. The magnitude of the resulting waveform at the simulator output terminals was then measured to obtain the output/input voltage ratio at various frequencies.

The open-loop response curves were obtained without feedback resistor R16, while the closed-loop response curve was obtained with R16 in the circuit.

The original open-loop response curve, shown in figure 6, indicated four major breakpoint frequencies. The first, at 300 Hz, was the result of the operational amplifier A1, a Philbrick type P65AU. Both the second and the third breakpoints, at 1 kHz and 30 kHz, were due to transistor Q3, a Westinghouse type 2N3430. A fourth breakpoint existed in the region of 200 kHz, although its cause was not determined. Consequently, a gain decrease of 60 db per decade resulted at the 14 db crossover. This caused closed-loop oscillations of approximately 200 kHz.

The system was stabilized as follows. The Q3 transistor type 2N3430 was replaced with an MHT6310. This eliminated the breakpoints at 1 kHz and 30 kHz. Furthermore, a feedback capacitor was introduced across operational amplifier A1. This lowered the first breakpoint frequency. Thus, the operational amplifier was the only frequency limiting component above unity gain. This resulted in a stable closed loop. The resulting closed loop frequency response curve is shown in figure 6. It exhibits a roll-off frequency of about 20 kHz, which dictates the frequency response capabilities of the simulator. These capabilities are completely valid only for smaller load excursions, however, since the operational amplifiers are rate-limited devices. Consequently, the 50-microsecond response time indicated in figures 7, 8 and 9 under various load conditions implies a closed-loop roll-off frequency of only 5 kHz.

The basic criterion for stable closed-loop operation is to ensure that a 180° signal phase shift does not occur when the gain is greater than unity (0db). This implies that the slope of the frequency response curve can not be greater than -20db/decade
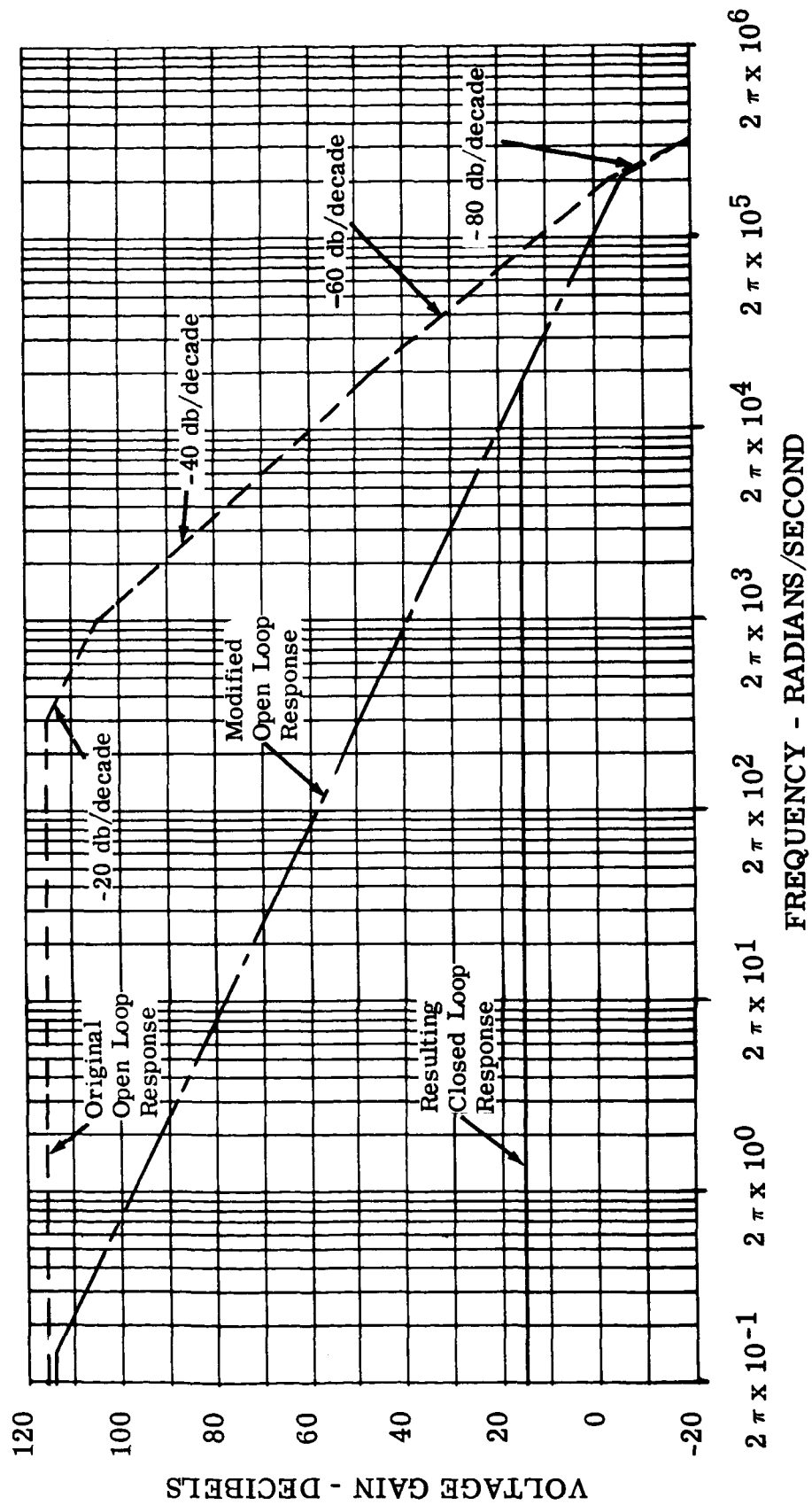
FIGURE 6. Frequency Response Curves of Simulator

11

FIGURE 7A. Simulator transient response at 1 kHz load switching frequency. Load switches between 11 and 17 amperes

Horizontal:  0.5 msec/cm
Vertical:    2.0 volts/cm



FIGURE 7B. Expansion of Figure 7A during load application

Horizontal:  50 $\mu$sec/cm
Vertical:    2.0 volts/cm



FIGURE 7C. Expansion of Figure 7A during load removal

Horizontal:  50 $\mu$sec/cm
Vertical:    2.0 volts/cm

FIGURE 8A. Simulator transient response at 1 kHz load switching frequency. Load switches between 10 and 20 amperes

Horizontal:   0.5 msec/cm
Vertical:      2.0 volts/cm



FIGURE 8B. Expansion of Figure 8A during load application

Horizontal:   50 $\mu$sec/cm
Vertical:      2.0 volts/cm



FIGURE 8C. Expansion of Figure 8A during load removal

Horizontal:   50 $\mu$sec/cm
Vertical:      2.0 volts/cm
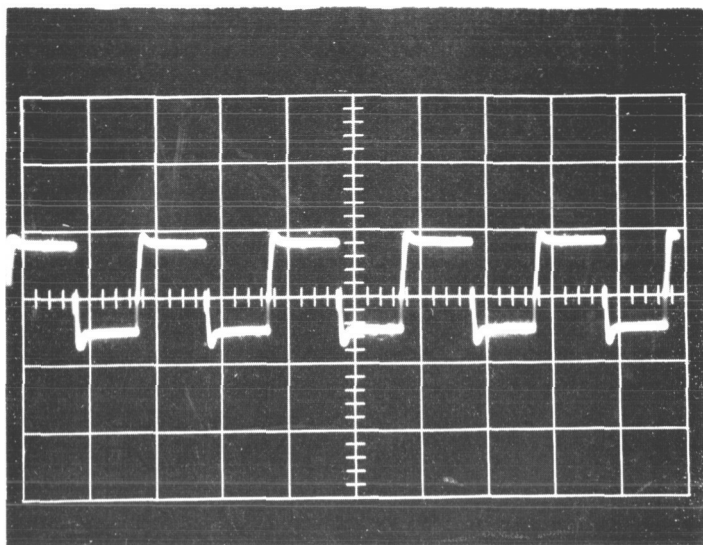
FIGURE 9A. Simulator transient response at 1 kHz load switching frequency. Load switches between 23 and 28 amperes

Horizontal: 0.5 msec/cm
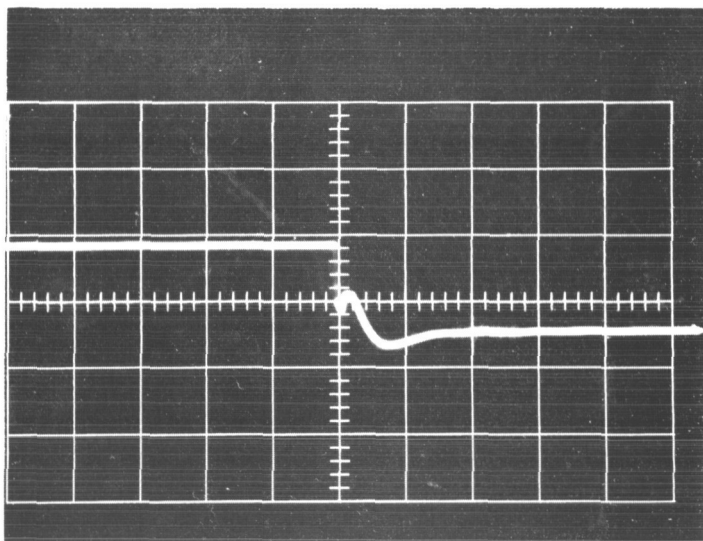Vertical: 2.0 volts/cm



FIGURE 9B. Expansion of Figure 9A during load application
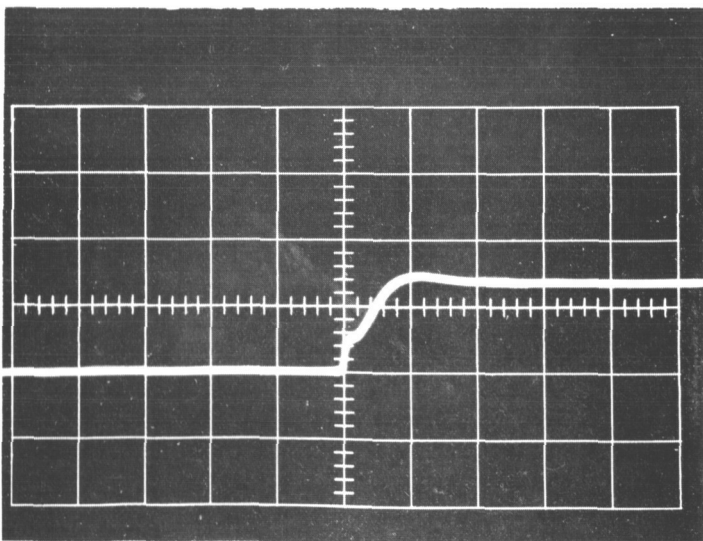
Horizontal: 50 $\mu$sec/cm
Vertical: 2.0 volts/cm
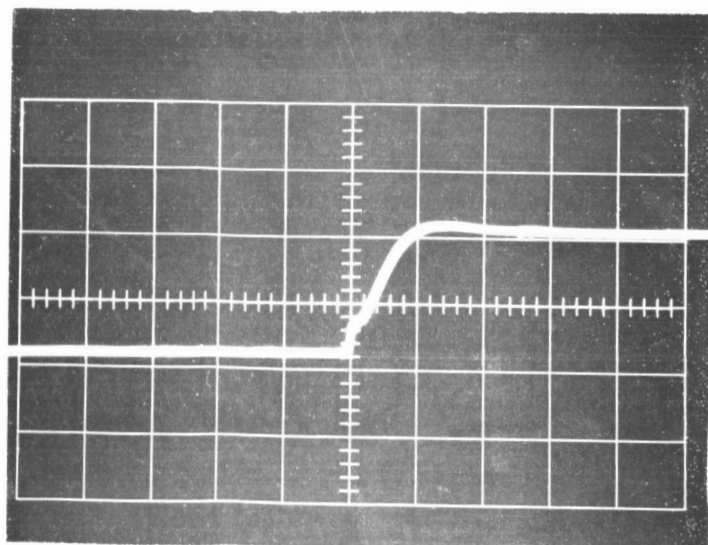


FIGURE 9C. Expansion of Figure 9A during load removal
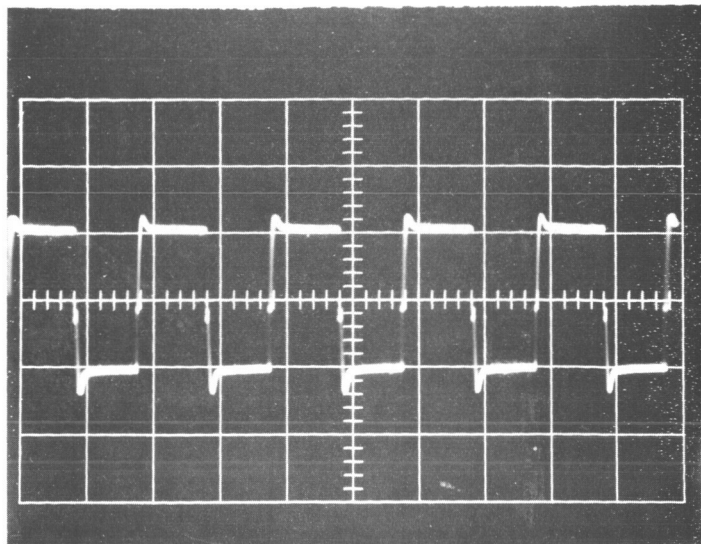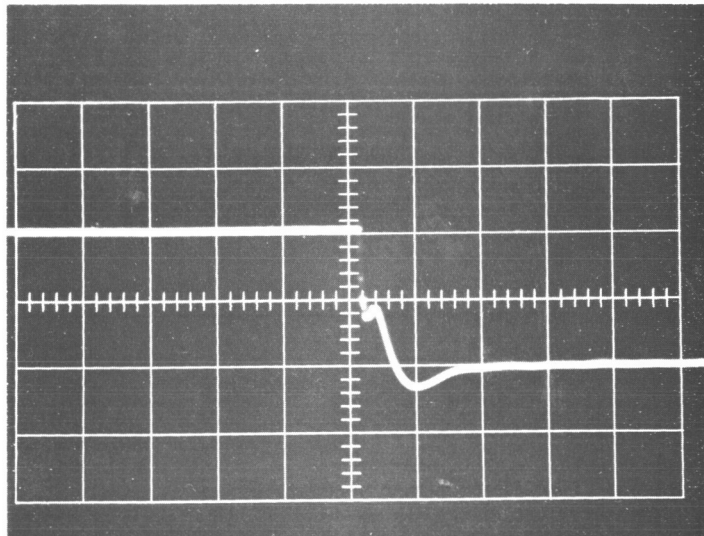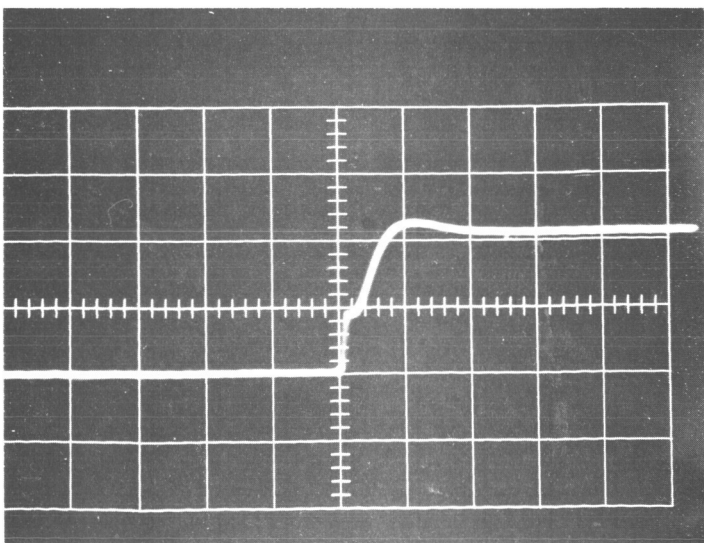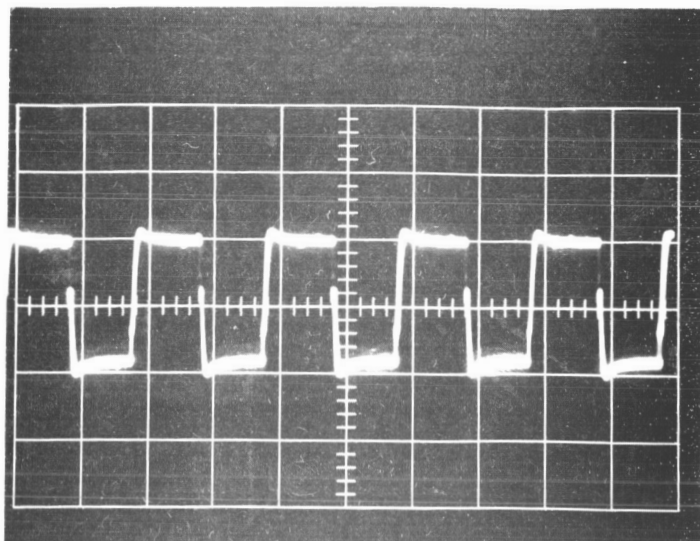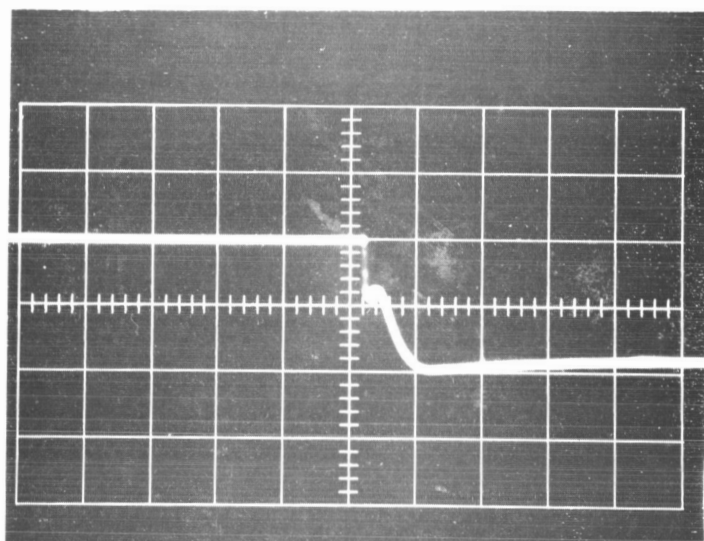
Horizontal: 50 $\mu$sec/cm
Vertical: 2.0 volts/cm

above 0db. The simulator meets these requirements as shown by the closed-loop response curve in figure 6.

In order to increase the simulator response time, it would be necessary to shift the open-loop response curve of figure 6 to the right, while ensuring a -20db/decade slope above 0db. It is apparent that the breakpoint at 200 kHz is the limiting factor in any such attempt. Furthermore, the cause of this breakpoint was not clearly defined, but appeared to be attributable to such factors as stray wiring capacitance, transistor junction capacitance, and the like. A prelude to increased response capabilities must therefore be the analysis of these types of factors, and would no doubt result in requiring extreme care in the location of components and associated wiring during fabrication of a unit.

The resultant response of the simulator to changing load is illustrated photographically in figures 7, 8 and 9 under various conditions. The response time is typically 50 microseconds.

## NOISE PROBLEMS

Electrical noise was a major concern in the design of the simulator. After stabilization, the d-c output was found to exhibit a considerable amount of undesired electrical noise. The prime sources of this noise were inductor L1 and the magnetic oscillator consisting of Q9, Q10, and associated components.

The inductor was located very close to current shunts R99 and R100. These shunts had been connected in series as shown in figure 10. Note that this connection formed a loop which was capable of producing a voltage when subjected to a changing electromagnetic field. This induced voltage was fed directly to operational amplifier A2. As a result of this injected signal, the ripple appearing at the output of the simulator was of such magnitude as to be unacceptable.

To reduce this effect as much as possible, the following action was taken. First, a non-inductive current shunt was obtained. This prevented the formation of a pickup loop since the output terminals were adjacent to each other. Second, the output of the shunt was increased by a factor of three in an attempt to increase the signal-to-noise ratio. The resulting configuration reduced the simulator noise output considerably. Figure 11 shows the resulting output ripple under various degrees of simulator loading.

15
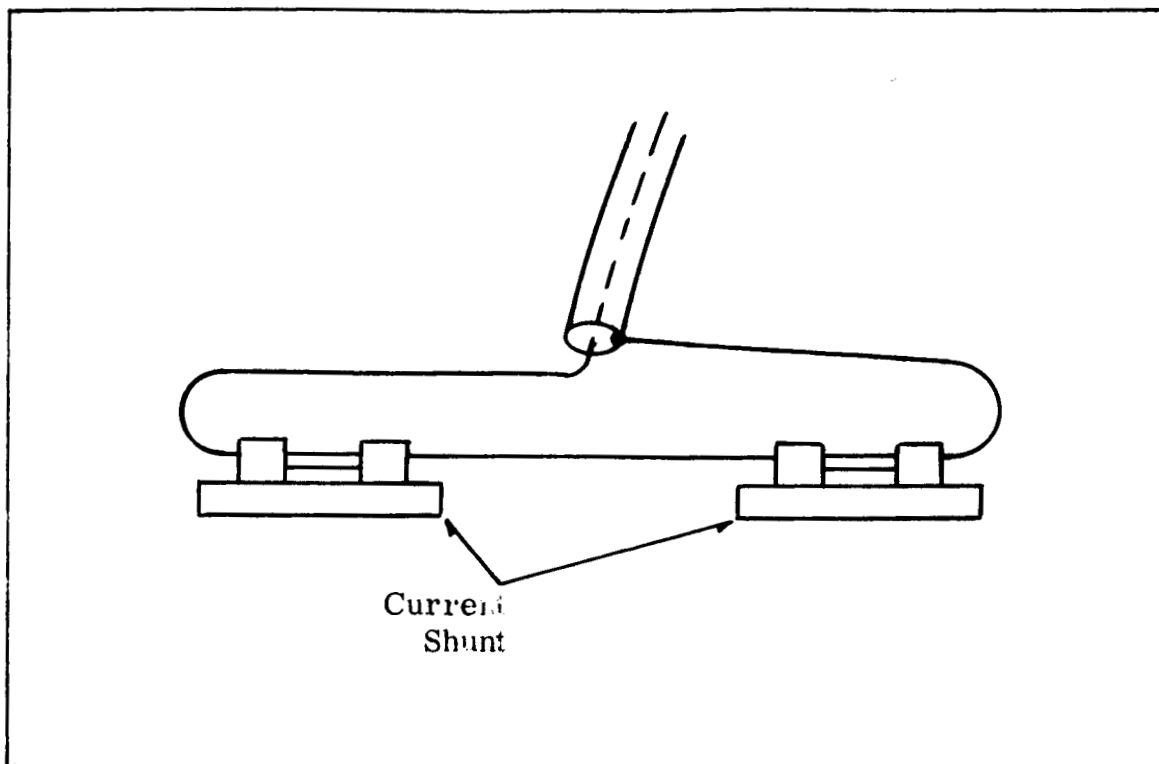
FIGURE 10.   Loop Formed by Series Connection
of Two Current Shunts

The noise injected into the system by the magnetic oscillator
required two distinct, corrective steps.  First, the entire oscil-
lator circuit board was shielded with an aluminum cover to pre-
vent radiated noise.  Second, the oscillator was isolated from
its power supply by means of an R-C filter in order to eliminate
the high rate-of-change of current in the power-supply line.  As
a result, the peak noise caused by the oscillator was reduced to
the extent that it did not exceed the peak noise already present
at the output and shown in figure 11.  Should it be desirable at
any time to disable the oscillator, an internal switch has been
provided for that purpose.  Disabling the oscillator removes the
protection feature of the power-limiting circuit to be described
in another section.  This feature, however, is only necessary
when double output is required from the simulator.


THE POWER DISSIPATION LIMITER


As described previously in this report, a power-dissipation lim-
iter was required in conjunction with the power transistors in

16
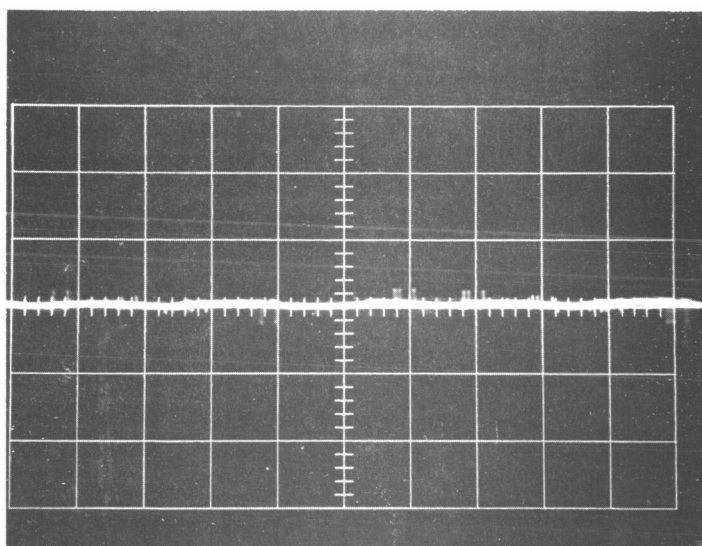
FIGURE 11A. Simulator output ripple under no-load conditions

Horizontal: 5.0 msec/cm
0.5 volts/cm
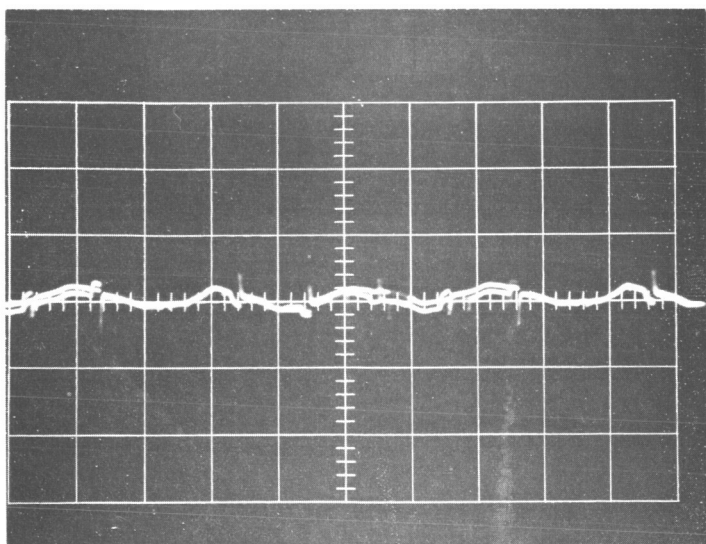


FIGURE 11B. Simulator output ripple with 27 amp load applied

Horizontal: 5.0 msec/cm
Vertical: 0.5 volts/cm

order to limit their number to twenty five. As evident from figure 1, however, the power limiting action is not necessary unless the simulator is required to deliver a short-circuit current exceeding 40 amperes. Referring to figure 2, the dissipation limiter senses the voltage across the power transistors by means of transformer T5, and the current through the power transistors by means of transformer T4. It utilizes a squarewave voltage source supplied by the magnetic oscillator in a configuration sometimes referred to as a transductor. Both transformers are merely saturable reactors which control the duration in which the square-wave is applied to the full-wave bridges. The duration is controlled in one case by the power-transistor voltage and in the other case by the power-transistor current. The resulting signals are rectified and filtered to produce voltages proportional to the variables being sensed. The two variables are then multiplied by allowing one to determine the pulse width, and the other the pulse amplitude of the collector voltage of transistor Q7. The average of the resulting waveform is proportional to the power dissipation in the main transistors. When this voltage exceeds that of reference diode CR29, base drive to the main transistors is reduced, such that the resulting output characteristic resembles that shown in figure 1.


## ADDITIONAL PROTECTIVE FEATURES


In addition to the power dissipation limiter, a number of safety features are incorporated in the simulator. Fuses protect both power transformers in the event of abnormal loading. A circuit breaker in series with the simulator output provides not only a convenient ON-OFF control, but protects the simulator in the event of a control circuit fault.

A free-wheeling diode, CR13, was incorporated to protect the simulator against any unusual transients which may occur during inductive load switching.

Likewise, diode CR11 protects the main power and driver transistors by allowing a capacitive-load discharge through transistor Q3. Should this discharge current exceed safe values, fuse F5 will open. This, in turn, will energize I5, resulting in a front panel indication of the fuse failure.

Thermostatic switches S3 and S4 are located on each of the forced-air cooled heatsinks. A failure of either of the main blowers will cause one of the switches to open, thereby interrupting base drive to the main transistors. Simultaneously, lamp I6 will be energized to provide a front panel indication. The thermostatic switches reset automatically as soon as the temperature returns to a safe level.

## MECHANICAL CONSIDERATIONS

Figure 12 shows a photograph of the simulator front panel. All controls were located for ease of access and readability, and were minimized for simplicity. Thus, the front panel contains a main power switch, an output circuit breaker, a control for open circuit voltage and a control for short circuit current.

Four green indicator lamps are energized when all input voltages are present, while two red indicator lamps are energized only under the abnormal conditions described previously.

Figures 13 and 14 show rear and top views of the simulator interior. The toggle switch located under the power receptacle in figure 13 selects one of two taps on the main power transformer to allow operation from 208-volt or 240-volt, 3-phase, 60-cycle power sources. An incorrect switch position is not harmful to the simulator, but may affect the output characteristics under certain load conditions. It is therefore important to maintain a check on the line-to-line voltage at periodic intervals.

The input connector includes a neutral connection and a chassis ground connection. The neutral connection may be connected, but is not necessary under normal conditions. Figure 14 shows a complete view of all fuses. Their location allows easy access for visual inspection and replacement.

## POSSIBLE IMPROVEMENTS

Several areas where improvements in operation may be realized should be considered at this time. These are as follows:

1. A revised layout of the simulator components should acknowledge those components and circuits which produce electrical noise as well as those which are susceptible to electrical noise. This action would further reduce the undesirable signals injected into the system such as those shown in figure 11.

2. A gain increase in the power-dissipation limiter loop should be considered, in order to allow limiter operation closer to the constant-power limit curve shown as a design objective in figure 2.

3. A detailed analysis of the uppermost breakpoint frequency shown in figure 6 would determine the cause of
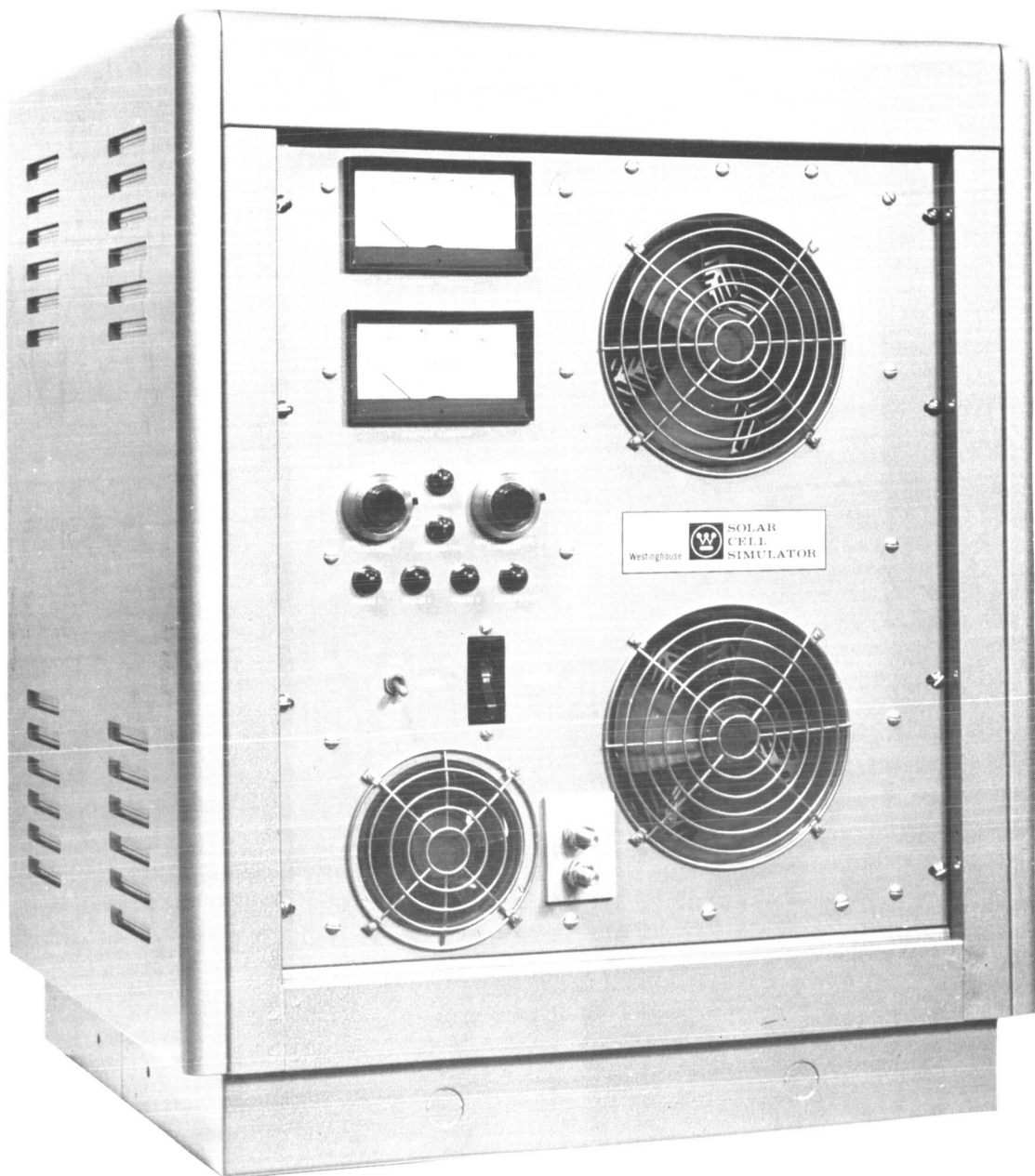
FIGURE 12.   Front View of Simulator
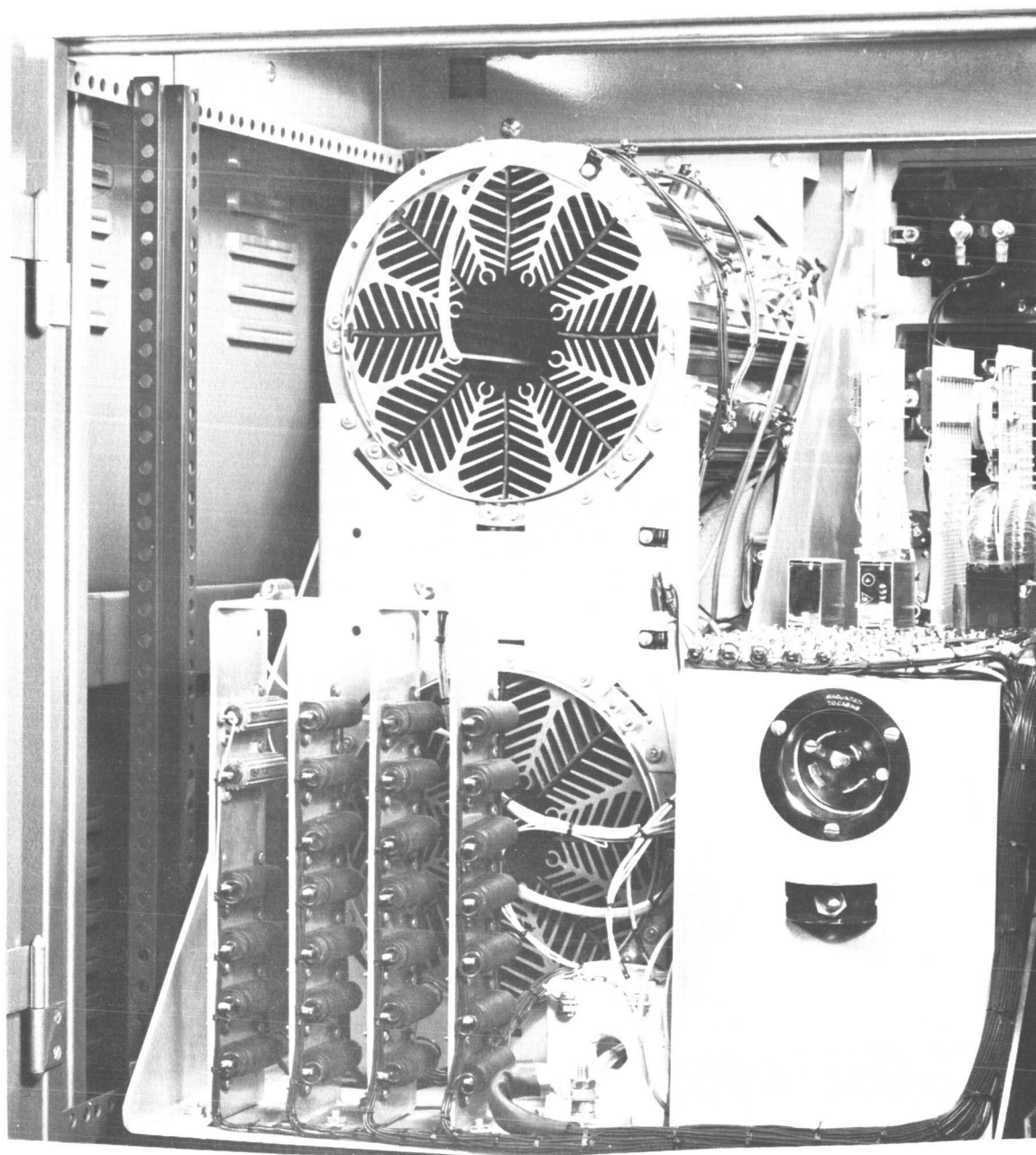
FIGURE 13.   Rear View of Simulator With Access Door Open
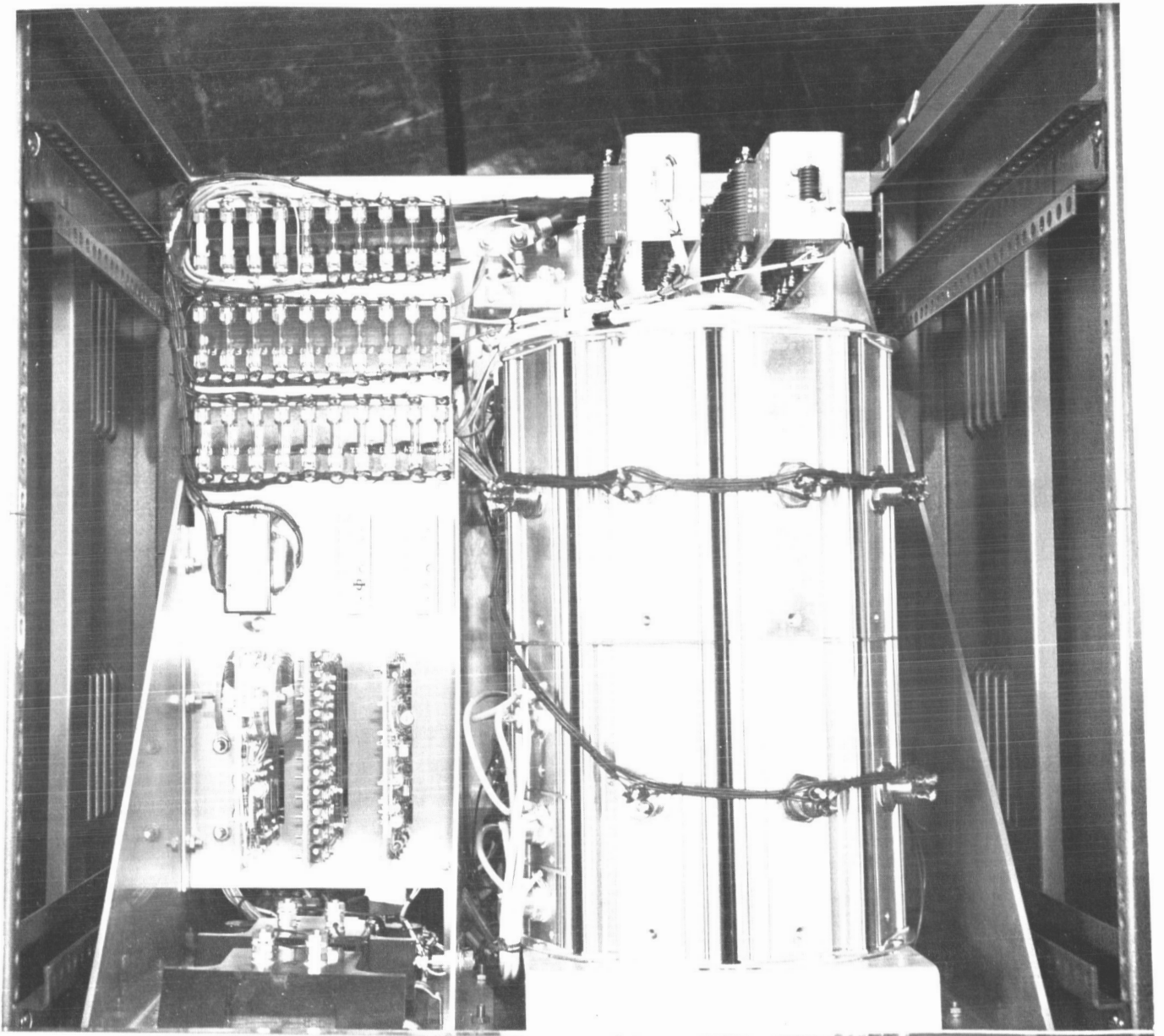
FIGURE 14.   Top View of Simulator With Access Door Open

22

this breakpoint, and would dictate what action is required to improve the closed-loop response of the simulator. The analysis should include the effect of wiring capacitance, especially in light of the present wiring arrangement, where the collector and base leads to the power transistors run parallel. This arrangement appears similar to the well known Miller-effect in vacuum tubes, where the effect of the plate-to-grid capacitance is multiplied by the gain of the device.

In any case, of course, the need for improvements must be considered in light of specific requirements.

## CONCLUSIONS

The principal objectives of this project were to develop a d-c power supply capable of simulating both the static and the dynamic characteristics of a solar-cell array. A major design problem was to obtain the transient response capability typical of a solar cell. To obtain a response of this magnitude required a very careful selection and placement of components to (a) make the system least susceptible to noise, and (b) to reduce the effects of stray capacitance.

Although slight improvements in such areas as frequency response could be obtained as discussed previously, it is believed that the simulation of solar-cell array characteristics to the extent accomplished by this simulator represents a state-of-the-art demonstration of power supply capabilities not previously attempted.

APPENDIX

PARTS LIST

| Reference Designation | Description |
|---|---|
| A1, A2 | Operational Amplifier |
| | Capacitors |
| C1A, C1B | 100 WVDC 2250 MFD |
| C2, C19 | 47 MFD 50V |
| C3A, C3B, C8 | 100 MFD 25V |
| C4, C5, C16 | 1 MFD 35V |
| C6, C7 | 1 MFD 150V |
| C12 | 1.5 MFD 50V |
| C9 | 1 MFD 220V |
| C10, C11 | 2 MFD 220V |
| C13, C14, C15 | 0.01 MFD |
| C17 | 200 PF |
| C18 | 0.0050 MFD |
| CB1 | Circuit Breaker - 90A |
| | Diodes |
| CR1, CR2, CR3, CR4, CR5, CR6 | 1N1184 |
| CR7, CR8, CR14, CR16, CR21-28, CR32-35, CR39-42 | 1N645 |
| CR9 | 1N3026B |
| CR10, CR15 | 1N3024B |
| CR11, CR13 | 1N1200 |
| CR30, CR38 | 8.2V Reference |
| CR29 | 4.7V Reference |
| CR37 | 1N2982B |
| | Fuses |
| F1-F3 | 20 amp |
| F4 | 1 amp |
| F5 | 0.125 amp |
| F101-F125 | 5 amp |
| I1-I4 | Lamp 110V |
| I5-I6 | Lamp 60V |
| J1 | Connector |
| L1 | Filter Choke |

| Reference Designation | Description |
|---|---|
| | Meters |
| M1 | 0-80V |
| M2 | 0-100V |
| | |
| P1 | Connector |
| | |
| | Transistors |
| Q1, Q101-Q125 | 2N2758 |
| Q2 | 2N3430 |
| Q4, Q6-Q11 | 2N2102 |
| Q5 | 2N3494 |
| Q3 | MHT 6310 |
| | |
| | Resistors |
| R1 | 10K Variable |
| R2 | 200K 1/2W CC |
| R3 | 12 1W CC |
| R40, R41 | 10K 1/2W CC |
| R5 | 51K 1/2W CC |
| R7, R27, R29, R54, R64 | 5.1K 1/2W CC |
| R8, R39 | 6.2K 1/2W CC |
| R9 | 51 1/2W CC |
| R10 | 10K Variable |
| R11, R20, R21 | 1 MEG Variable |
| R12, R22 | 500K Variable |
| R13, R23 | 250K Variable |
| R14, R24 | 50K Variable |
| R15, R25, R44 | 5K Variable |
| R16 | 1 MEG 1/2W CC |
| R17, R33 | 39K 1/2W CC |
| R34 | 3K 1/2W CC |
| R19 | 230 OHM 20W WW |
| R26 | 100 1/2W CC |
| R28, R62 | 510 1/2W CC |
| R30 | 50K Variable |
| R38 | 300 1/2W CC |
| R31 | 27K 1/2W CC |
| R35 | 1100 5W WW |
| R36 | 5000 1W WW |
| R37 | 2K 1W CC |
| R60 | 11K 1/2W CC |
| R42, R52 | 20K 1/2W CC |
| R45 | 75 5W WW |
| R46 | 200 1W CC |
| R47, R49, R43, R59 | 2K 1/2W CC |
| R48 | 1K 10W WW |
| R50 | 200 1/2W CC |
| R51 | 91 1W CC |

| Reference Designation | Description |
|---|---|
| | Resistors (Cont.) |
| R53, R66-R70 | 100 50W WW |
| R55 | 10 1/2W CC |
| R56 | 30K 1/2W CC |
| R57 | 510K 1/2W CC |
| R65 | 50K Variable |
| R61 | 18K 1/2W CC |
| R6 | 1K 1/2W CC |
| R4 | 7.5K 1/2W CC |
| R63 | 3.9K 1/2W CC |
| R32 | 820 1/2W CC |
| R71 | 20 OHMS 1W CC |
| R72 | 47 OHMS 1W CC |
| | |
| R99 | Non-Inductive Shunt 100A 300 MV |
| | |
| R100 | Shunt 100A 50 MV |
| | |
| R101-R125 | Resistor 3 OHMS 50W WW |
| | |
| | Switches |
| S1 | 4PST |
| S2 | 4PDT |
| | |
| S3,S4 | Thermostat 90° C |
| | |
| S5 | Switch SPST |
| | |
| | Transformers |
| T1 | Main Power |
| T2 | Auxiliary Power |
| T3 | Magnetic Oscillator |
| T4 | Current Sensing |
| T5 | Voltage Sensing |
| | |
| | Blowers |
| B1, B2 | Heat Sink |
| B3 | Transformer |

## DISTRIBUTION LIST FOR SUMMARY REPORT

### Contract NAS3-7920

National Aeronautics and Space Administration
Washington, D. C.  20546
Attn:  RNT/James Lazar  (1)
       RNW/Preston T. Maxwell  (1)

NASA-Lewis Research Center
21000 Brookpark Road
Cleveland, Ohio  44135
Attn:  B. L. Sater  M.S. 54-3  (4)
       J. R. Eski  M.S. 54-2  (1)
       R. D. Shattuck  M.S. 54-3  (1)
       Jesse Hall  M.S. 77-1  (1)
       C. S. Corcoran, Jr.  M.S. 500-201  (1)
       F. Gourash  M.S. 500-201  (1)
       V. R. Lalli  M.S. 500-203  (1)
       J. J. Weber  M.S. 3-16  (1)
       C. C. Conger  M.S. 54-1  (1)
       C. W. Knoop  M.S. 54-3  (1)
       Library  M.S. 60-3  (2)
       Reports Control Office  (M.S. 5-5)  (1)
       Office of Reliability and Quality
          Assurance  M.S. 500-203  (1)

NASA Scientific and Technical Information Facility  (6)
P. O. Box 33
College Park, Maryland  20740
Attn:  NASA Representative RQT-2448

NASA Ames Research Center  (1)
Moffett Field, California  94035
Attn:  Library

NASA Flight Research Center  (1)
P. O. Box 273
Edwards, California  93423
Attn:  Library

NASA Goddard Space Flight Center
Greenbelt, Maryland  20771
Attn:  Library  (1)
       Robert L. Weitzel  (1)
       Fred C. Yagerhofer  (1)

Jet Propulsion Laboratory
4800 Oak Grove Drive
Pasadena, California  91103
Attn:  Library  (1)
       Jack Sterns  (1)


NASA Langley Research Center  (1)
Langley Station
Hampton, Virginia  23365
Attn:  Library


NASA Manned Spacecraft Center  (1)
Houston, Texas  77001
Attn:  Library


NASA Marshall Space Flight Center
Huntsville, Alabama  35812
Attn:  Library  (1)
       Robert Harwell  (1)
       Joseph Parker  (1)


NASA Western Operations  (1)
150 Pico Boulevard
Santa Monica, California  90406
Attn:  Library                          '


AFWL  (1)
Kirtland Air Force Base, New Mexico  87417
Attn:  Capt. C. F. Ellis/ WLPC


Aerospace Corporation  (1)
P. O. Box 95085
Los Angeles, California  90045
Attn:  Library Technical Documents Group


Westinghouse Astronuclear Laboratories  (1)
Pittsburgh, Pennsylvania  15234
Attn:  Library


Westinghouse Electric Corporation
Aerospace Electrical Division
P. O. Box 989
Lima, Ohio  45802
Attn:  Library  (1)
       H. B. James  (1)

Westinghouse Electric Corporation    (1)
P. O. Box 10596
Pittsburgh, Pennsylvania    15235
Attn:  A. H. B. Walker

Electro-Optical Systems, Inc.    (1)
125 N. Vinedo Avenue
Pasadena, California    91107
Attn:  John Davis

General Electric Company    (1)
Speciality Control Department
Waynesboro, Virginia    22980
Attn:  Army L. Wilford

TRW Inc.    (1)
Electromechanical Division
23555 Euclid Avenue
Cleveland, Ohio    44117
Attn:  Paul H. McGarrell

Hughes Research Laboratories    (1)
3011 Malibu Canyon Road
Malibu, California    93032
Attn:  Dr. George R. Brewer

TRW Inc.    (1)
TRW Systems Group
One Space Park
Redondo Beach, California    90278
Attn:  Dr. F. Kraus

Hughes Aircraft Company (1)
Century Blvd.
Los Angeles, California
Attn:  W. J. Muldoon

NASA-Electronics Research Center
575 Technology Square
Cambridge, Massachusetts    02039
Attn:  Library    (1)
        Dr. Frederick Niemann    (1)

Duke University
Durham, North Carolina  27706
Attn:  Dean, College of Engineering  (1)
       Dr. Thomas G. Wilson, Chairman E.E. Dept.  (1)

U. S. Army Electronics Laboratory  (1)
Power Conditioning Sion
Ft. Monmouth, New Jersey
Attn:  Mr. Frank Wrublewski